



Effects of cross rolling on texture, mechanical properties and anisotropy of pure Mo plates

De-zhi WANG^{1,2}, Yao-xin JI¹, Zhuang-zhi WU^{1,2}

1. School of Materials Science and Engineering, Central South University, Changsha 410083, China;

2. Key Laboratory of Ministry of Education for Non-ferrous Materials Science and Engineering,
Central South University, Changsha 410083, China

Received 21 November 2019; accepted 20 May 2020

Abstract: To clarify the influence of the deformation texture on the mechanical properties, pure Mo plates were processed by various cross rolling procedures, and the relation among texture, microstructure and mechanical properties was discussed. The results show that cross rolling of the Mo plates is beneficial for the formation of the rotated cube component, i.e., $\{001\}\langle 110\rangle$. The corresponding orientation density exhibits a positive correlation with the total rolling deformation and the current-pass deformation. When the total deformation is 96% or greater, the Mo plates form a texture orientation dominated by $\{001\}\langle 110\rangle$, whereas the γ -fibre texture becomes weaker and the cube texture $\{100\}\langle 100\rangle$ disappears completely. The presence of $\{001\}\langle 110\rangle$ has great effects on the properties of cross-rolled Mo plates, which is beneficial for strength enhancement and plasticity reduction in both the rolling direction (RD) and the transverse direction (TD).

Key words: Mo plates; cross rolling; tensile strength; texture; anisotropy

1 Introduction

Molybdenum (Mo) is a body-centered rare refractory metal with a high melting point, high strength, high modulus of elasticity, low expansion coefficient, and outstanding electrical and thermal conductivity [1–4]. Mo and its alloys have been widely used in the metallurgy, military, electronics and steel industries [5–8]. Rolled Mo plates are important products in the field of Mo processing, and texture has a substantial influence on the mechanical performance of these plates. FUJII et al [9] studied the effects of rolling and annealing processes on grain changes and texture evolution in pure and doped molybdenum. OERTEL et al [10,11] reported that straight rolling generated α -fibre textures with a maximum at $\{100\}\langle 110\rangle$, and the

maximum shifted to $\{112\}\langle 110\rangle$ at higher rolling degrees; in contrast, cross rolling formed a texture orientation dominated by the rotated cube component $\{100\}\langle 110\rangle$. They also used the Taylor–Bishop–Hill theory to qualitatively explain the plastic anisotropy of the sheets. CHAUDHURI et al [12] found that $\langle 001\rangle$ fibre textures became stronger during dynamic recrystallization. YOU [13] summarized that Mo plates formed α -fibre textures with cold rolling reduction of 30%–60% and γ -fibre textures with reduction of 70%–80%. When the reduction reached 90%, the (001) textures were weakened, whereas the (111) textures were strengthened.

At present, most related researches focus on the evolution of textures, and there are few studies on the effects of cross rolling deformation on the correlation between the mechanical properties and

Foundation item: Project (2017YFB0306001) supported by the National Key R&D Program of China; Project (502221802) supported by the Innovation-Driven Project of Central South University, China

Corresponding author: Zhuang-zhi WU; Tel: +86-13974889625; E-mail: zww2012@csu.edu.cn

DOI: 10.1016/S1003-6326(20)65369-9

texture evolution of pure Mo plates. In this work, pure Mo plates were obtained by different cross rolling processes, and the corresponding textures and mechanical properties were determined. The anisotropy of the tensile strength of these plates was also analyzed and discussed from the perspective of grain orientation, which would provide a theoretical basis for the development of high-performance Mo plates.

2 Experimental

Typically, the original Mo powders (3 μm) were pressed into plates with a thickness of 30 mm at 250 MPa for 60 s. Then, the plates were sintered at 1900 °C in hydrogen for 4 h. The grain size of the sintered plates was approximately 50 μm , and the texture was nearly random. The chemical composition of the Mo plates is given in Table 1. Rolling experiments were carried out by various cross rolling processes, and the obtained samples were named A1, A2, B1 and B2. First, all of the Mo plates were hot-rolled from 30 to 19 mm at a starting temperature of 1400 °C. Then, the plates were subjected to reverse rolling. The Plates A were hot-rolled to 4.5 mm, whereas the Plates B were hot-rolled to 3 mm. Finally, Mo plates with thicknesses of 2 and 1 mm were obtained by warm rolling at a starting temperature of 900 °C. The flow chart of cross rolling is shown in Fig. 1. All plates were annealed at 800 °C for 1 h after rolling.

Table 1 Chemical composition of starting Mo billets (wt.%)

O	N	C	Fe	Ni	Si	Mo
0.0048	0.0035	0.0066	0.003	0.002	0.002	Bal.

According to Fig. 1, both A1 and A2 were cross-rolled from 4.5 to 2 mm, and then A2 was further cross-rolled from 2 to 1 mm. Moreover, B1 and B2 were cross-rolled from 3 to 2 and 1 mm, respectively. After rolling, the tension test samples were taken in the rolling direction (RD), transverse direction (TD) and 45° to the rolling direction (45°D). These samples, which had a gauge length of 50 mm, were subjected to tension tests on a universal testing machine (Instron 8802) at a crosshead displacement rate of 2 mm/min.

There were a total of 24 tension test samples,

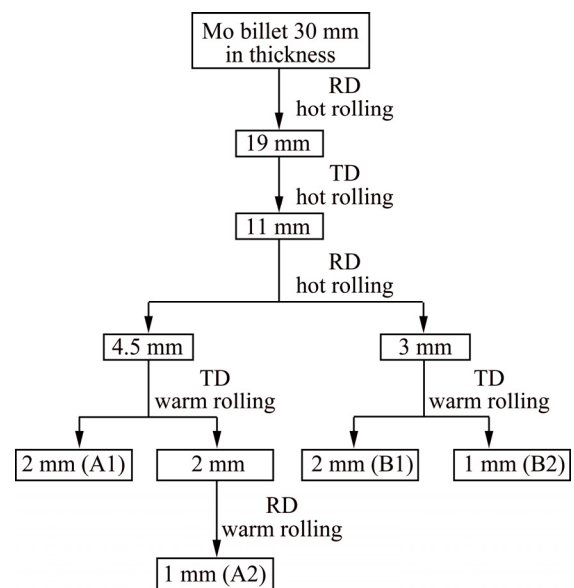


Fig. 1 Flow chart of cross rolling

among which two parallel samples were taken from each plate. Hardness tests were conducted on an HVS-1000 Vickers hardness tester with a load of 0.3 kg and a dwell time of 15 s. Five hardness measurements were taken for each sample, and the average value was determined. The microstructures were observed with a Leica DMIL LED inverted microscope. The texture measurements were performed on the surface and centre of the plates, which were prepared by mechanical polishing. The pole figures of (110), (200) and (211) were obtained with a Bruker X-ray texture stress metre (D8 Discover) using Cu K_{α} radiation, which were analyzed by relevant software to determine the corresponding orientation distribution function (ODF) patterns and the diagrams of orientation lines that characterized the texture.

3 Results and discussion

3.1 Effects of cross rolling on texture

The ODF patterns were obtained by detecting and analyzing the surface texture of the four rolled Mo plates. Cross-sectional views of constant $\varphi_2=45^\circ$ are shown in Fig. 2. All the Mo plates exhibit a strong rotated cube component, which is $\{001\}\langle 110\rangle$ with coordinates $(0^\circ, 0^\circ, 45^\circ)$, when the Mo plates are rolled to 2 mm. In addition, continuous α -fibre and γ -fibre textures, including $\{111\}\langle 110\rangle$ and $\{111\}\langle 112\rangle$, and a cube texture, i.e., $\{001\}\langle 100\rangle$, are found. When the Mo plates are

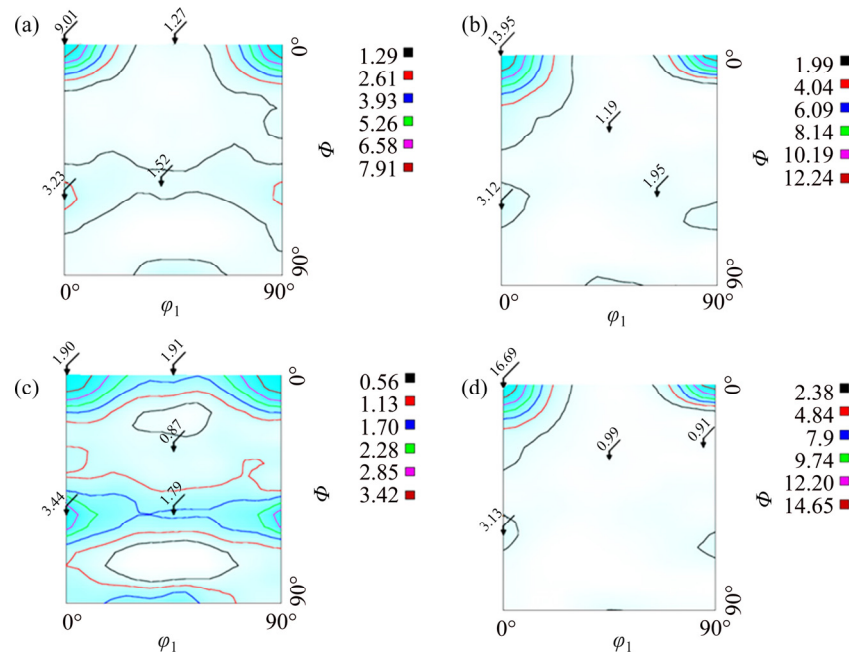


Fig. 2 ODF patterns of Mo plates at constant $\varphi_2=45^\circ$: (a) A1; (b) A2; (c) B1; (d) B2

rolled to 1 mm, the orientation density of $\{001\}\langle 110\rangle$ increases from 9.01 in A1 to 13.95 in A2 and increases from 3.90 in B1 to 16.69 in B2. Furthermore, both α -fibre and γ -fibre textures become discontinuous. The orientation intensities of the textures, including $\{111\}\langle 110\rangle$ and $\{111\}\langle 112\rangle$, are not remarkably changed but become weaker than the $\{001\}\langle 110\rangle$ texture. The cube texture disappears completely. When the total deformation is 96% or greater, the Mo plates form a texture orientation dominated by $\{001\}\langle 110\rangle$. The $\{001\}\langle 110\rangle$ orientation density of A1 is stronger than that of B1, and that of B2 is stronger than that of A2. The other components have similar trends.

According to Figs. 1 and 2, the orientation density of $\{001\}\langle 110\rangle$ is also related to the rolling deformation of the current pass. In the last reverse rolling step, the reduction rates of A1 and B1 were 55.6% and 33.3%, respectively, whereas the reduction rates of A2 and B2 were 50.0% and 66.7%, respectively. Therefore, the orientation density of $\{001\}\langle 110\rangle$ in A1 is higher than that in B1, whereas the orientation density of $\{001\}\langle 110\rangle$ in A2 is lower than in B2. Moreover, the $\{001\}\langle 110\rangle$ enhancement in B1 and B2 is greater than that in A1 and A2. Evidently, it can be concluded that the density of $\{001\}\langle 110\rangle$ is directly proportional to the deformation degree. $\{HKL\}\langle uvw\rangle$ and $(\varphi_1, \Phi, \varphi_2)$ are two expressions of texture orientation, and the conversion formulas

between them are shown as follows [14]:

$$H:K:L = \sin \Phi \sin \varphi_2 : \sin \Phi \cos \varphi_2 : \cos \Phi \quad (1)$$

$$u:v:w = (\cos \varphi_1 \cos \varphi_2 - \sin \varphi_1 \sin \varphi_2 \cos \Phi) : (-\cos \varphi_1 \sin \varphi_2 - \sin \varphi_1 \cos \varphi_2 \cos \Phi) : \sin \varphi_1 \sin \Phi \quad (2)$$

In these formulas, $(0^\circ, 0^\circ, 45^\circ)$, $(90^\circ, 0^\circ, 45^\circ)$ and $(0^\circ, 54.7^\circ, 45^\circ)$ correspond to $(001)[1\bar{1}0]$, $(001)[110]$ and $(111)[1\bar{1}0]$, respectively. According to Fig. 2, the grain orientations are concentrated at $(001)[1\bar{1}0]$ and $(001)[110]$, while weak $(111)[1\bar{1}0]$ also exists.

Figure 3 shows the orientation density variation of the textures. These results intuitively indicate that the grain orientation of the Mo plates generally tends to evolve and aggregate towards $\{001\}\langle 110\rangle$ and that the 0° – 30° α -fibre textures are obviously strengthened with the increase in total rolling deformation. Other α -fibre textures still exist but are weaker. The orientation density values of the γ -fibre textures are nearly below 2, and the 70° – 90° γ -fibre textures are slightly reduced with a higher deformation degree.

According to the ODF patterns in Fig. 2, the evolution process of grain orientation during cross rolling is depicted in Fig. 4. The slip direction of Mo is $\langle 111\rangle$, and the slip planes are usually $\{110\}$ and $\{112\}$ [13,15]. The rolling process of Mo causes the slip system of $\{110\}\langle 111\rangle$ to start first according to the Schmid's law [16,17]. Then, other

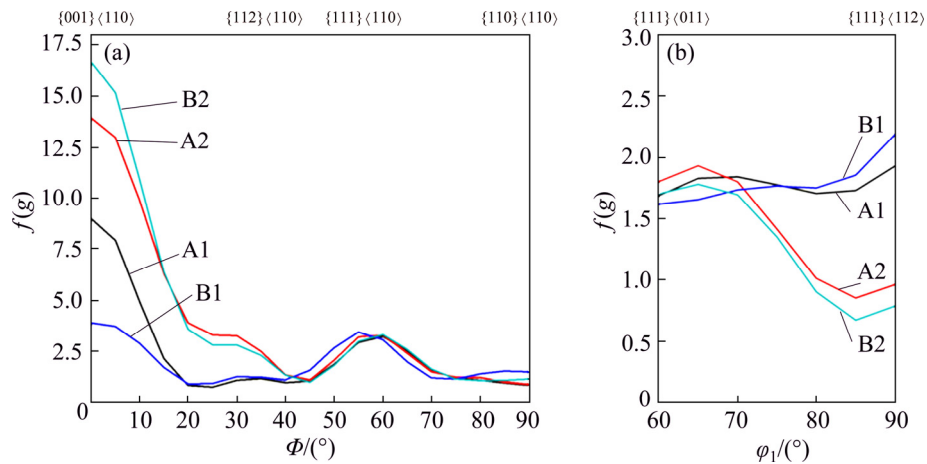


Fig. 3 Orientation lines of α -fibre (a) and γ -fibre (b) textures

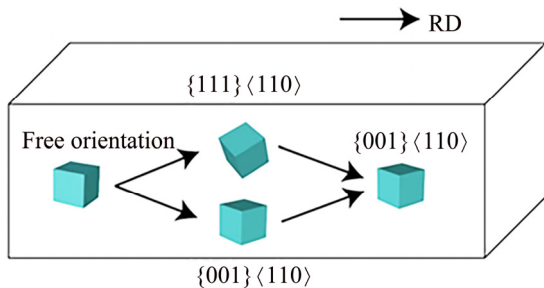


Fig. 4 Illustration of grain orientation evolution during cross rolling

slip systems are also activated due to the increased deformation resistance. The grains are changed from the original free orientation to produce textures during cross rolling, including $\{111\}\langle 110\rangle$, $\{111\}\langle 112\rangle$ and $\{001\}\langle 110\rangle$. Finally, a grain orientation dominated by $\{001\}\langle 110\rangle$ is obtained. Figure 4 reveals that the orientation of $\{001\}\langle 110\rangle$ is along the $\langle 110\rangle$ crystal orientation of the grains in both RD and TD.

3.2 Microstructure

The microstructures of the RD–TD sections of all the Mo plates are shown in Fig. 5. Some grains are homogeneous with a quasi-spherical shape, and most of grains are elongated along the RD and TD during cross rolling. There are few differences in the microstructures between the RD and TD, making the stress and strain distribution uniform [18].

3.3 Effects of cross rolling on mechanical properties

The Vickers hardness of the four samples was measured, and the results are shown in Fig. 6. This

figure shows that the hardness values of Plates A and B are increased by 3.7% and 9.6%, respectively, which can be attributed to the work hardening with a higher deformation degree. Figure 7 shows the relationship among the tensile strength, elongation and sampling direction for the Mo plates with the same thickness. All the Mo plates exhibit only a slight anisotropy with the lowest tensile strength and the highest elongation along the 45°D and the highest tensile strength and the lowest elongation along the TD.

The in-plane anisotropy (IPA) index is one of the characteristic indexes for anisotropy, for which the formula is expressed as follows [19,20]:

$$\text{IPA} = \frac{\{[(N-1)X_{\max} - X_{\text{mid}1} - X_{\text{mid}2} - X_{\text{mid}(N-2)} - X_{\min}]\}}{[(N-1)X_{\max}]} \times 100\% \quad (3)$$

where N is the number of sampling directions, which is 3, and X_{\max} , X_{\min} and X_{mid} are the maximum, minimum and intermediate values of tensile strength (σ_b) in the sampling direction, respectively. The calculated results are shown in Fig. 8. The IPAs of all the plates are relatively low ($<10\%$), indicating that the cross rolling process can effectively reduce the anisotropy of tensile strength in the Mo plates. For the Plates A, the IPA of A2 is lower than that of A1 due to the additional cross rolling process. For the Plates B, the deformation of B2 in the last reverse rolling pass is much greater than that of B1, which creates an obvious discrepancy in strength enhancement in different directions, as confirmed by B2 having a much higher IPA than B1.

In addition, regarding the plates with the same thickness, the hardness and tensile strength of A1

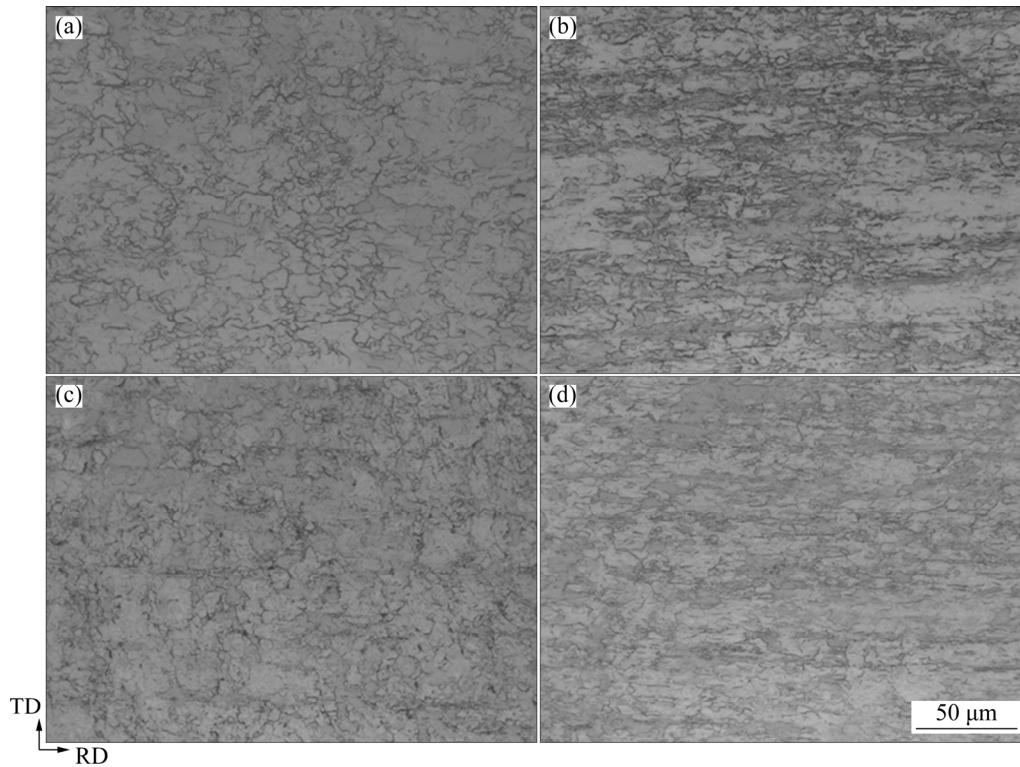


Fig. 5 Optical images of Mo plates in RD–TD sections: (a) A1; (b) A2; (c) B1; (d) B2

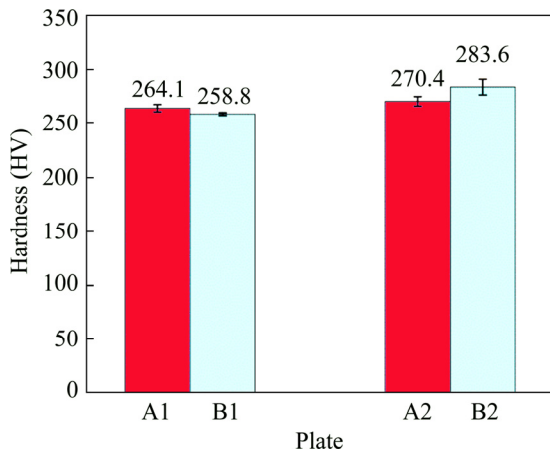


Fig. 6 Vickers hardness of rolled Mo plates

are higher than those of B1 and the hardness and tensile strength of A2 are lower than those of B2 in both the RD and TD; the elongation evolution exhibits the opposite trend. A1 and B2 store more deformation energy and a stronger degree of work hardening because these plates sustain greater deformation in the last reverse rolling pass. Furthermore, the trends in hardness, tensile strength, and elongation are very similar in the 45°D as a result of the 90° cross rolling step. High intensities of the γ -fibre textures are beneficial for good isotropy [11]. As a result, B1 and A2 show a

better isotropy than A1 and B2 (Fig. 8), which is consistent with the results shown in Fig. 3(b). However, the correlation between γ -fibre texture and isotropy is still not strong.

Crystallographic texture is the main source of anisotropy [21–24]. In the grains with an orientation of $\{001\}\langle 110\rangle$, the crystal orientation of $[110]$ corresponds to the RD, the crystal orientation of $[1\bar{1}0]$ is consistent with the TD and the crystal orientation of $[100]$ is along the 45°D. The tensile strength values in the TD and RD are close and are obviously higher than that in the 45°D. Moreover, the descending order of elongation rate is 45°D>RD>TD. From Fig. 3(a) and Fig. 7, it can be seen that the orientation density of $\{001\}\langle 110\rangle$ and the mechanical properties in the three directions have obvious correlations. Therefore, we can conclude that the rolled Mo plates have a relatively high intensity along the $\langle 110\rangle$ crystal orientation and a low intensity along the $\langle 100\rangle$ crystal orientation. The presence of $\{001\}\langle 110\rangle$ is beneficial for increasing the strength and decreasing the plasticity in the RD and TD. In conclusion, to obtain a higher tensile strength and elongation rate, $\langle 110\rangle$ and $\langle 100\rangle$ crystal orientations are preferred, respectively.

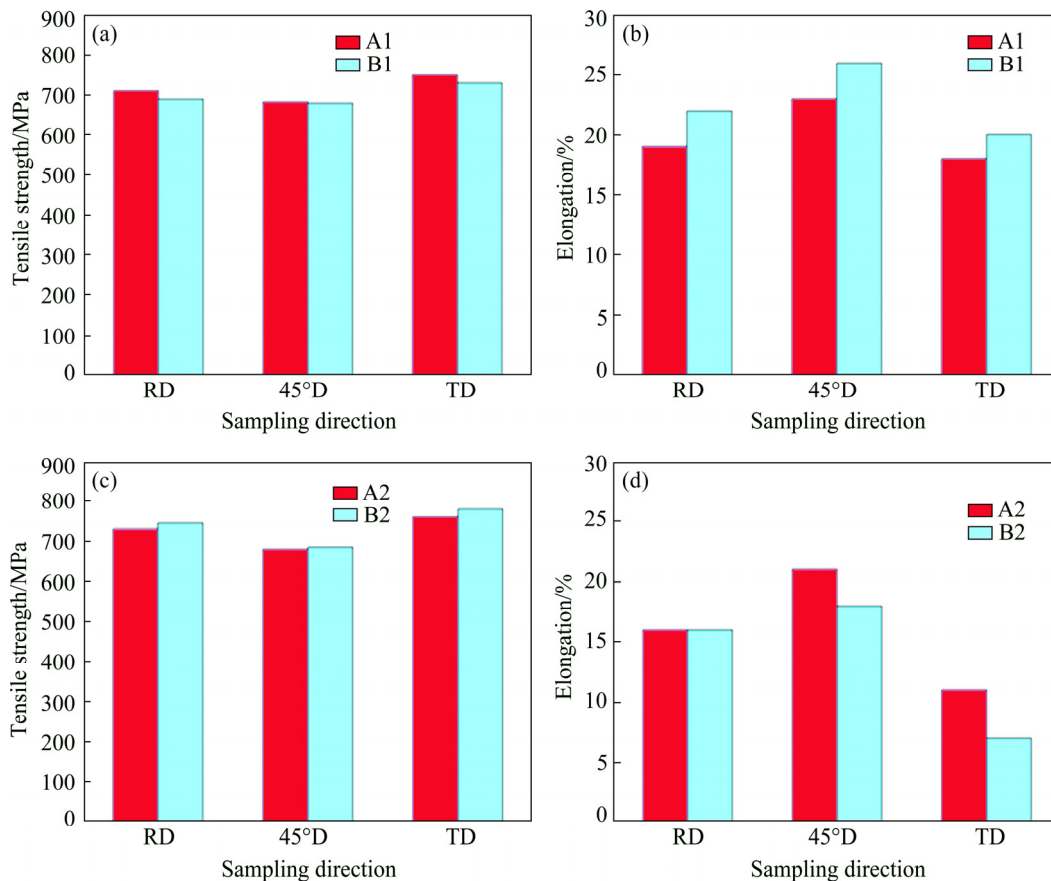


Fig. 7 Tensile strength (a, c) and elongation (b, d) of plates in various sampling directions: (a, b) A1 and B1; (c, d) A2 and B2

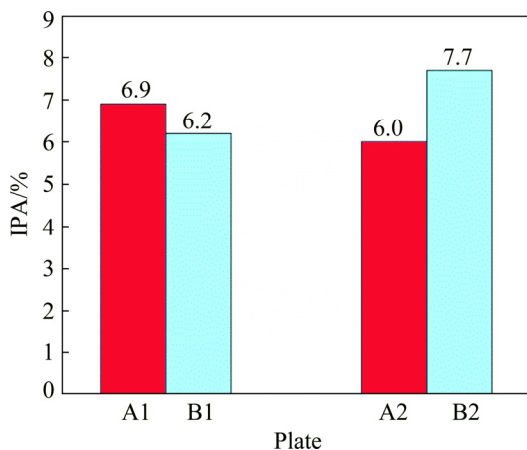


Fig. 8 IPA values of tensile strength of rolled Mo plates

4 Conclusions

(1) In the cross rolling process, Mo plates produce α -fibre, γ -fibre and cube textures at a lower deformation. The orientation density of the rotated cube component, i.e., $\{001\}\langle 110\rangle$, shows a positive correlation with the total rolling deformation and the deformation of the current pass. When the total deformation is 96% or greater, the grain orientation is dominated by $\{001\}\langle 110\rangle$, whereas the γ -fibre

texture becomes weaker and the cube texture $\{100\}\langle 100\rangle$ disappears completely.

(2) The presence of $\{001\}\langle 110\rangle$ in Mo plates is beneficial for increasing the strength and reducing the plasticity in both the RD and TD. In addition, $\langle 110\rangle$ and $\langle 100\rangle$ crystal orientations are preferred for increasing the tensile strength and elongation rate, respectively.

References

- [1] CAO Yuan-kui, LIU Yong, ZHANG Wei-dong, WANG Jia-wen, DU Meng. Effect of Al and Mo on high temperature oxidation behavior of refractory high entropy alloys [J]. Transactions of Nonferrous Metals Society of China, 2019, 29: 1476–1483.
- [2] FAN Xiao-hui, DENG Qiong, GAN Min, CHEN Xu-ling. Roasting oxidation behaviors of ReS_2 and MoS_2 in powdery rhenium-bearing, low-grade molybdenum concentrate [J]. Transactions of Nonferrous Metals Society of China, 2019, 29: 840–848.
- [3] YANG Song-tao, LI Ji-wen, WEI Shi-zhong, XU Liu-jie, ZHANG Guo-shang, ZHANG Er-zhao. Pyroplastic deformation behavior of pure molybdenum sheet and constitutive equation [J]. The Chinese Journal of Nonferrous Metals, 2011, 21: 2126–2131. (in Chinese)

- [4] DUAN Bo-hua, ZHANG Zhao, WANG De-zhi, ZHOU Tao. Microwave sintering of Mo nanopowder and its densification behavior [J]. Transactions of Nonferrous Metals Society of China, 2019, 29: 1705–1713.
- [5] WU Zhuang-zhi, LIU Xin, WANG De-zhi. Synthesis of high-performance Mo–La₂O₃ powder by hydrogen reduction of MoO₂ originated from a self-reduction strategy [J]. Materials Research Express, 2019, 6: 126586.
- [6] HU Ping, ZHOU Yu-hang, CHANG Tian, YU Zhi-tao, WANG Kuai-she, YANG Fan, HU Bo-liang, CAO Wei-cheng, YU Hai-liang. Investigation on compression behavior of TZM and La₂O₃ doped TZM alloys at high temperature [J]. Materials Science and Engineering A, 2017, 687: 276–280.
- [7] YILDIRIM M, AKDENIZ M V, MEKHRABOV A O. Effect of Mo addition on microstructure, ordering, and room-temperature mechanical properties of Fe–50Al [J]. Transactions of Nonferrous Metals Society of China, 2018, 28: 1970–1979.
- [8] KIM J M, HA T H, PARK J S, KIM H G. Oxidation resistance of Si-coated TZM alloy prepared through combined process of plasma spray and laser surface melting [J]. Transactions of Nonferrous Metals Society of China, 2016, 26: 2603–2608.
- [9] FUJII T, WATANABE R, HIRAOKA Y, OKADA M. Effects of rolling procedures on the development of annealing textures in molybdenum plates [J]. Journal of the Less Common Metals, 1984, 97: 163–171.
- [10] OERTEL C G, HUNSCHE I, SKROTZKI W, KNABL W, LORICH A, RESCH J. Plastic anisotropy of straight and cross rolled molybdenum plates [J]. Material Science and Engineering A, 2008, 483–484: 79–83.
- [11] OERTEL C G, HUNSCHE I, SKROTZKI W, LORICH A, KNABL W, RESCH J, TRENKWALDER T. Influence of cross rolling and heat treatment on texture and forming properties of molybdenum plates [J]. Int J Refract Met Hard Mater, 2010, 28: 722–727.
- [12] CHAUDHURI A, SARKAR A, SUWAS S. Investigation of stress–strain response, microstructure and texture of hot deformed pure molybdenum [J]. Int J Refract Met Hard Mater, 2018, 73: 168–182.
- [13] YOU Shi-wu. Investigation of textures in cold-rolled pure Mo plates [J]. Physical Testing and Chemical Analysis (Part A): Physical Testing, 2000, 36: 342–344.
- [14] BUNGE H J. Texture analysis in material science [M]. London: Butterworths, 1982.
- [15] TAN Wang, CHEN Chang, WANG Ming-pu, JIA Yan-lin, XIA Fu-zhong, XIA Cheng-dong. Effects of texture and microstructure on transverse ductility of pure molybdenum bars in upset process [J]. The Chinese Journal of Nonferrous Metals, 2010, 20: 859–865. (in Chinese)
- [16] NI Heng-fei, ZHANG Guo-huan, YAN Ming-gao. Influence of the grain orientation on the strength and fracture at elevated temperature in a directionally-solidified superalloy, DZ5 [J]. Aeronautical Materials, 1981, 1: 1–7.
- [17] NGAN A H W, WEN M. Dislocation kink-pair energetics and pencil glide in body-centered-cubic crystals [J]. Physical Review Letters, 2001, 87: 075505.
- [18] WEI Xiu-yu. Effects of cross rolling on microstructure and formability of molybdenum sheet [J]. Cemented Carbide, 2017, 34: 97–102.
- [19] SINGH R K, SINGH A K, PRASAD N E. Texture and mechanical property anisotropy in an Al–Mg–Si–Cu alloy [J]. Material Science and Engineering A, 2000, 277: 114–122.
- [20] JATA K V, HOPKINS A K, RIOJA R J. The anisotropy and texture of Al–Li alloys [J]. Materials Science Forum, 1996, 217–222: 647–652.
- [21] WALDE T. Plastic anisotropy of thin molybdenum sheets [J]. Int J Refract Met Hard Mater, 2008, 26: 396–403.
- [22] ZADERII B A, KOTENKO S S, MARINCHENKO A E, POLISHCHUK E P, YUSHCHENKO K A. Anisotropy of mechanical properties in deformed molybdenum alloy sheets [J]. Strength of Materials, 2005, 37: 566–572.
- [23] RAABE D, LUCKE K. Rolling and annealing textures of BCC metals [J]. Materials Science Forum, 1994, 157–162: 597–610.
- [24] PARK Y B, LEE D N, GOTTSTEIN G. The evolution of recrystallization textures in body centered cubic metals [J]. Acta Materialia, 1998, 46: 3371–3379.

交叉轧制对纯钼板织构、力学性能及各向异性的影响

王德志^{1,2}, 姬耀鑫¹, 吴壮志^{1,2}

1. 中南大学 材料科学与工程学院, 长沙 410083;

2. 中南大学 有色金属材料科学与工程教育部重点实验室, 长沙 410083

摘要: 为了研究变形织构对力学性能的影响, 对纯钼板进行不同工艺的交叉轧制, 然后表征所得钼板的织构、力学性能和显微组织。结果表明: 交叉轧制有利于钼板形成旋转立方织构, 即{001}⟨110⟩织构, 其取向密度随着轧制总变形量和当前道次变形量的增大而增大; 当轧制总变形量达到 96%或更高时, 钼板会形成以{001}⟨110⟩织构为主导的晶粒取向, 而纤维织构变弱, 同时立方织构{001}⟨100⟩完全消失。{001}⟨110⟩织构的存在有利于交叉轧制钼板轧制方向和垂直轧制方向的强度提高和塑性降低。

关键词: 钼板; 交叉轧制; 拉伸强度; 织构; 各向异性